SATELLITE RADIANCE ASSIMILATION IMPACT IN NEW CANADIAN ENSEMBLE-VARIATIONAL SYSTEM

Louis Garand, Mark Buehner, Sylvain Heilliette, Stephen R. MacPherson, and Alain Beaulne

Environment Canada, 2121 Trans-Canada Highway, Dorval, Qc, Canada, H9P1J3

Abstract

The impact of satellite radiances is reassessed in the context of the upcoming ensemble-variational data assimilation system at Environment Canada, which benefits from a flow-dependent background error covariance matrix. Data denial experiments, consisting of removing either microwave or infrared radiances, confirm the large positive impact from both observation types. The impact in forecasts is further increased by doubling the number of assimilated hyperspectal IR channels (142 each for AIRS and IASI), and optimizing the assigned observation error and bias correction procedure. Impact evaluation is also evaluated from degrees of freedom (DFS) statistics pertaining to various observation types and individual channels.

INTRODUCTION

Environment Canada's operational deterministic data assimilation system is currently based on a 4D-var approach (Gauthier et al., 2007). Environment Canada also provides probabilistic forecasts from an Ensemble Kalman Filter (EnKF) system (see Houtekamer et al., 2013 for latest developments). A major change to the deterministic system is planned for 2014: the implementation of an ensemble-variational (EnVar) system in replacement of 4DVar. The analysis remains variational, but the system benefits from a flow-dependent background error covariance matrix provided by the EnKF. Significant efficiency is gained by eliminating the need to fit the trajectory of the model using its adjoint. Results obtained so far are convincing (Buehner et al., 2013).

The goal of this study is to reassess the impact of radiances in that new context where the background covariance matrix differs substantially. Notably, the humidity analysis becomes multivariate while it was univariate before. This implementation is also an occasion to further optimize the assigned observation error pertaining to radiances, review the bias correction procedure, and increase substantially the number of assimilated infrared channels from AIRS and IASI.

CHANNEL SELECTION AND BIAS CORRECTION

Table 1 shows the current distribution of AIRS (87) and IASI (62) channels, and that planned for EnVar (142 in each). Previous studies indicated that such a distribution captures the essential information content linked to temperature and humidity. About thirty high peaking temperature channels are added. IASI water vapor channels (33) now contribute at the same level as AIRS. The number of assimilated channels is not a limiting factor in EnVar, thanks to parallelization. With thinning of radiances at 150 km, the number of assimilated IR (AIRS and IASI) and MW (AMSU-A/B and MHS) radiances is currently 1.2 M/day and 2.6 M/day, respectively. With the added IR channels and same thinning, the number of assimilated IR radiances will reach 3.8 M/day. With EnVar, the resolution of the analysis will improve from 66 Km to 50 km, while that of the forecast model will increase from 25 km to 15 km. Tests will be conducted to further reduce the thinning, resulting in a significant increase of assimilated radiances. EnVar tests presented here are based on the 66/25 km resolutions.

cm-1	Spectral bands	4DVar		EnVar	
		AIRS	IASI	AIRS	IASI
650-770	T sounding (peak higher than 80mb)	0	0	0	0
	T sounding (80mb < peak < 150mb)	0	0	28	30
	T sounding (peak lower than 150mb)	20	43	34	45
770-980	Surface, low peaking T, RH sounding	6	19	12	19
980-1070	Ozone sounding	0	0	0	0
1070-1310	Surface and cloud properties	4	0	8	6
1310-2035	Water vapor & temperature sounding	33	0	32	33
2035-2175	CO column amount	0	0	0	0
2175-2250	Temperature sounding (N2O band)	9	0	13	9
2250-2420	Temperature sounding (CO2 Band)	15	0	15	0
2420-2700	Surface and cloud properties	0	0	0	0
	Total	87	62	142	142

Table 1. Current (4DVar, and tested (EnVar) distribution of assimilated AIRS and IASI channels.

The radiance bias correction (BC) is done offline based on the last 7 days of data. Predictors evolve dynamically except for AMSU-A 13 and 14 where the bias correction parameters are fixed to avoid temperature drift near the model top. BC predictors are now the same for all radiances: four geopotential thicknesses. The intent is to minimize the possibility of conflicts between IR and MW forcings induced by the bias correction. Another modification is that BC predictors are refreshed at 00 UTC and 12 UTC based on observed minus analysis differences obtained from a 3DVar analysis (instead of observed minus background differences) produced separately (from EnVar background) and excluding radiances. This is done to give more weight to data considered less biased such as GPS-RO and radiosondes.

IMPACT IN ENVAR

Test were conducted from 2-month long assimilation cycles (5 Feb. to 31 March 2011) to assess the impact of radiances in EnVar. These were done with the current configuration of channels (87 AIRS, 62 IASI). The control experiment used all data. The test consisted in removing either IR (AIRS, IASI, GEO), or MW radiances (AMSU-A/B, MHS), keeping SSMI. The result is shown in Fig.1. The positive impact at day 5 for global data is clearly positive for the four variables shown over most of the atmosphere. The impact is more evident for MW radiances, in part due to their higher volume. Fig. 2, in turn, compares the impact of adding either IR or MW radiances to a control without these radiances (NORAD). In that light, the impact is very large, and comparable for IR and MW radiances, although the MW impact remains slightly higher. These experiments confirm the strong impact of radiances in EnVar, similar to that seen in 4DVar (not shown). These cycles used the revised observation errors define below.

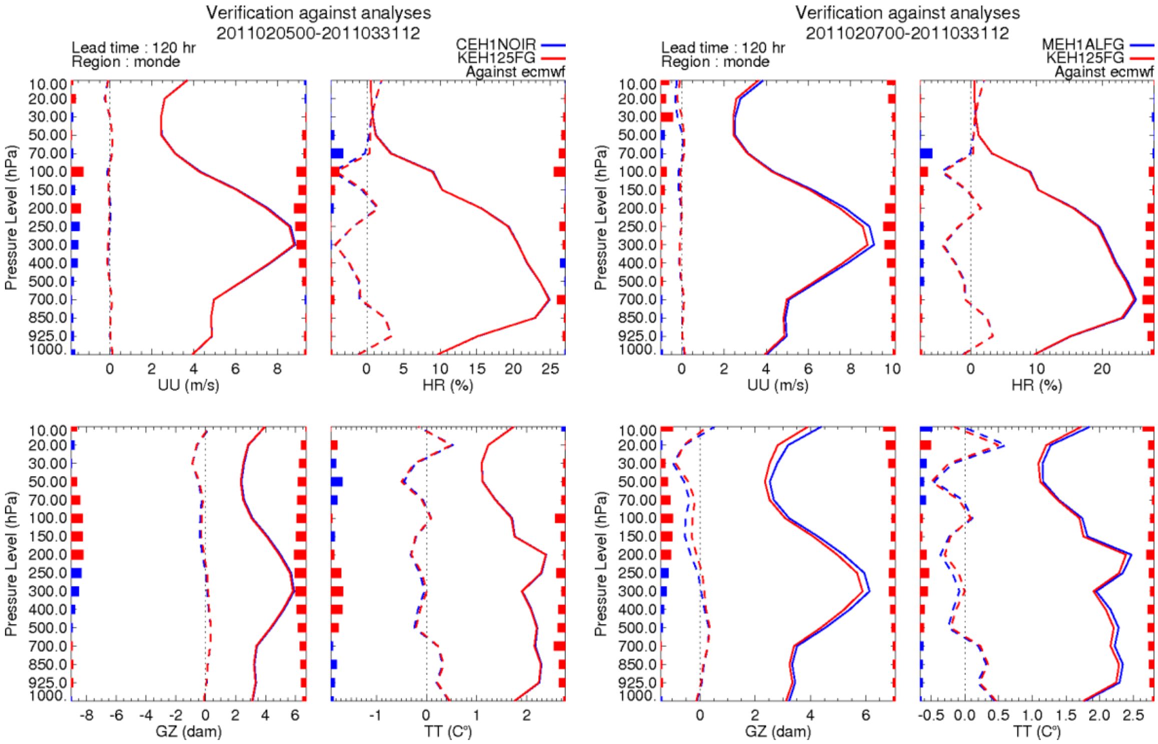

***Figure 1**:* Global 120-h statistics of standard deviations (full lines) and bias (dashed lines) of experiments without infrared (left, blue) or microwave (right, blue) radiances evaluated against ECMWF analyses, in comparison to an experiment using all data (red). Statistics shown as a function of level for the four variables indicated. Relative differences shown by blocks scaled to highest difference (red denotes positive impact).

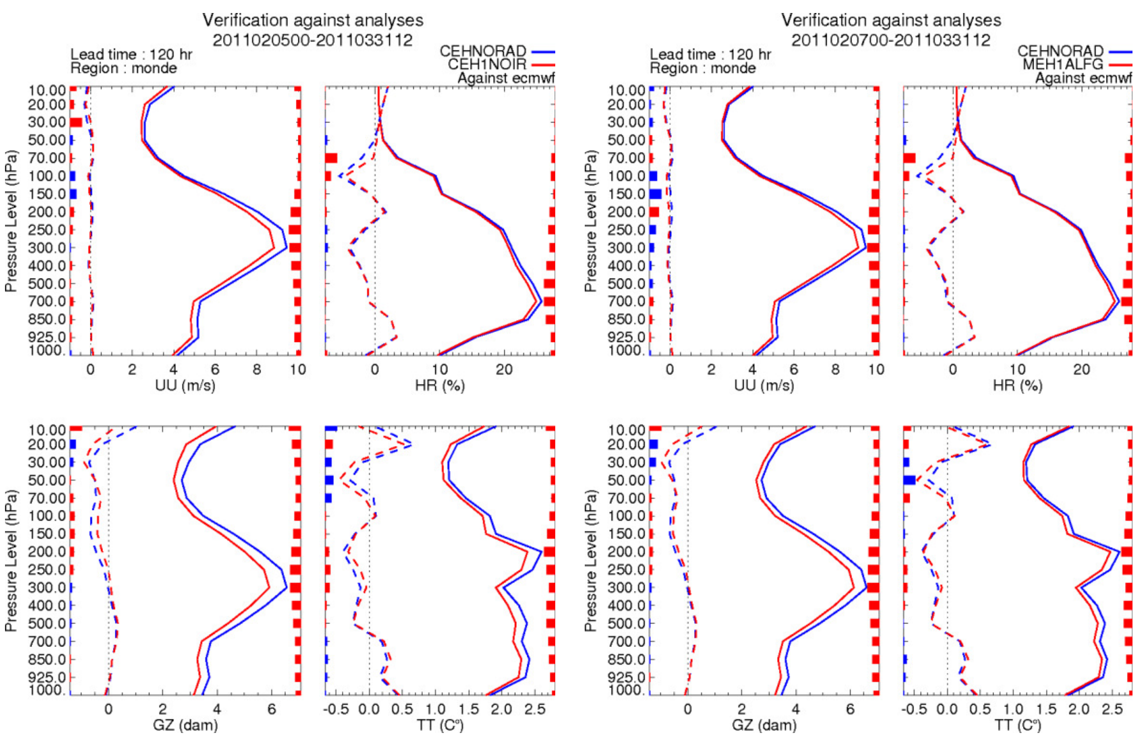

***Figure 2**:* Same as Fig. 1 except that the control is defined by no AIRS/IASI radiances (NORAD, blue), and the experiments by NORAD + MW (left, red), and NORAD + IR (right, red).

OBSERVATION ERROR DEFINITION

The radiance observation error cannot be established once for all. It requires revision as the assimilation configuration evolves (new data, thinning, forward model, background error), which affects spatial, temporal, and interchannel error correlations. Here, we adopted a simple approach, where the observation error is defined by a factor F, which in general depends on channel, times std(O-P), with O the observation and P the predicted (6-h background) value. We proceeded by sensitivity experiments in short cycles. It is possible using the adjoint of the model to objectively evaluate the sensitivity of the forecast error to the assigned observation error, as shown by Daescu and Langland (2013). That approach provides qualitative information on the direction to modify the observation error. These authors found, for example, that in their system, the error associated to IR data should be increased, while that due to AMSU-A radiances should be decreased. We obtained a similar result, as shown in Fig. 3. Our F factors for IR data were originally close to 1. The figure displays std(O-P), the assigned observation error, and its estimate from the Desroziers diagnostic, i.e., E<(O-P)(O-A)>, where A is the analysis in observation space (Desroziers et al., 2005); E denotes expected value. F varies typically between 1.1 and 2.0. For high peaking AMSU-A channels 11-14, F is larger, providing more weight to GPS-RO data. Yet, the assimilation remains strong for these channels (difference between std(O-P) and std(O-A), not shown). For temperature channels, the Desroziers estimate follows closely std(O-P). This is not the case for surface and water vapor channels. This is related to the fact that the assimilation system does not consider interchannel error correlation (Garand et al. (2007). Even if it did, it is anticipated that the optimum observation error would remain inflated to take into account a remaining representativeness error and spatio-temporal error correlations. For AMSU-B and SSMI/S, the F factor was set to 2. For AIRS and IASI, F is set to 1.6 for temperature channels, and to 2.0 for all other channels. It is planned to use in assimilation a full observation error covariance matrix for all radiances, as opposed to the current diagonal matrix, which will require a new revision of inflation factors.

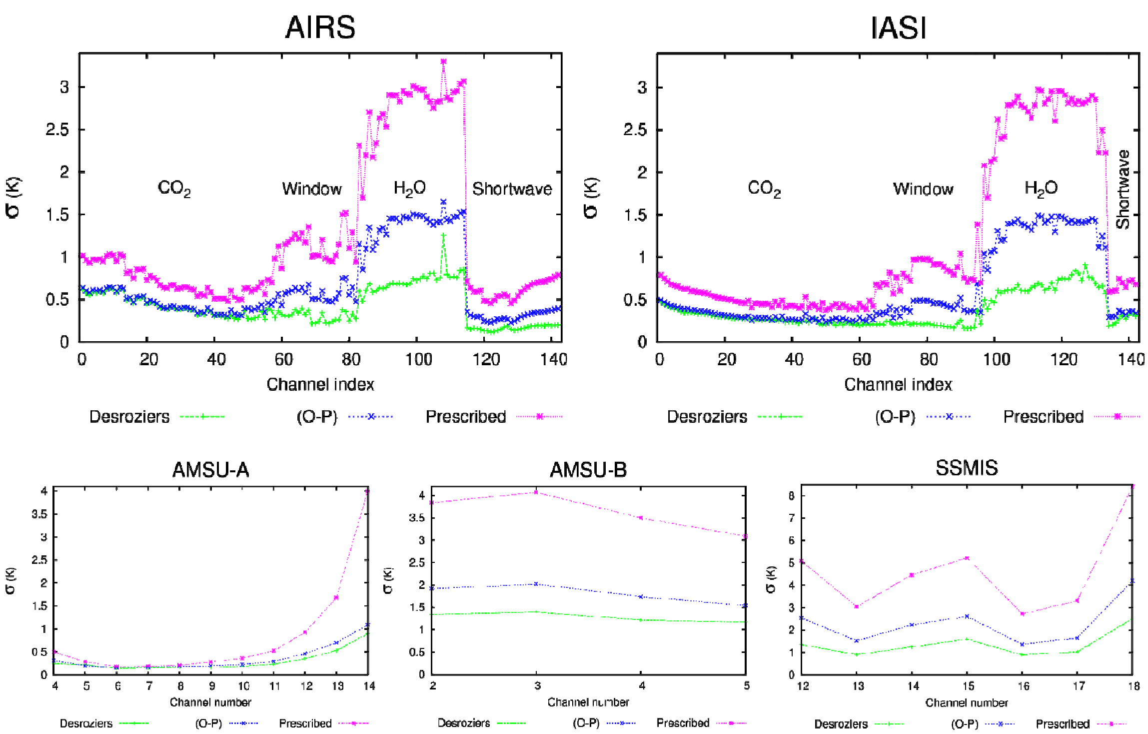

Fig.3*:* Assigned observation error (purple), std of observed minus 6-h brightness temperatures (blue), and Desroziers estimate of observation error (green) for AIRS, IASI, AMSU-A/B, ad SSMIS assimilated channels. Units: K.

ADDING AIRS AND IASI CHANNELS

Fig. 4 shows the impact at day 5 of adding a substantial amount of AIRS and IASI channels (142 for each, see Table 1). The result is shown for the Southern Hemisphere extratropics (20-70° S). The positive impact is clear for most of the atmosphere for the four variables shown. The impact in the Northern Hemisphere was neutral. A positive impact in all regions was noted for upper level humidity. Based on these results, the new set of channels will be part of the EnVar implementation planned for mid 2014. In the mean time, tests will be carried out to possibly reduce the thinning from 150 km to 100 km, which, if conclusive, would more than double the number of assimilated radiances.

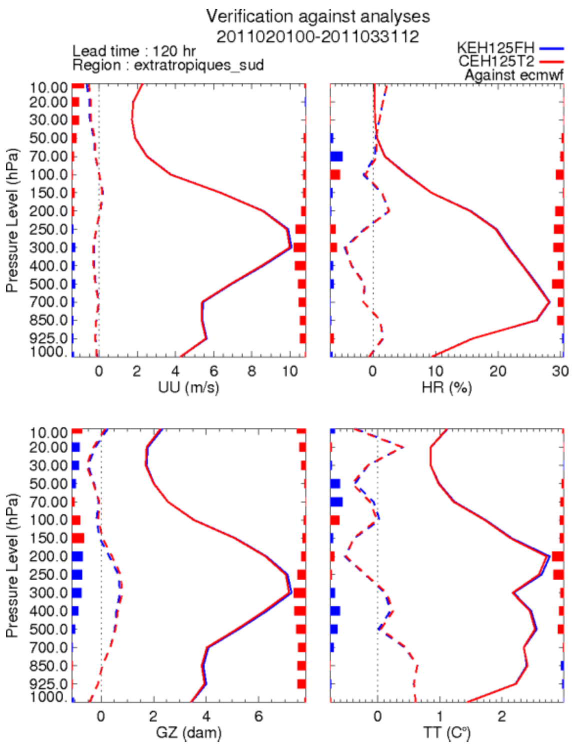

Fig. 4. As in Fig. 1, showing the impact at day 5 of assimilating more AIRS and IASI channels (red) versus a control experiment (blue) with the current set of channels (see Table 1). Region is Southern Hemisphere extratropics.

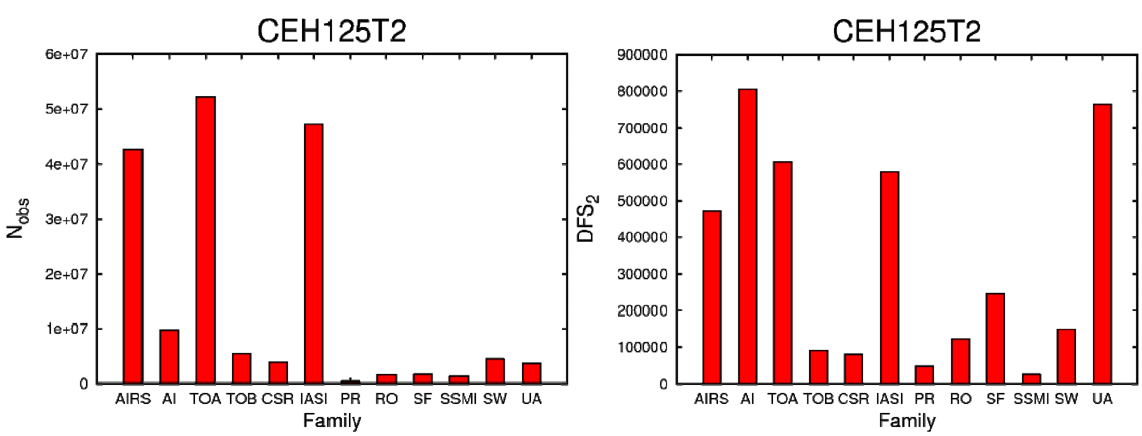

Fig. 5 : Number of observations in a 23-day period assimilated in each family (left) and corresponding DFS (right). AI: aircaft, TOA: AMSU-A, TOB: AMSU-B, PR: profilers, RO:GPS-RO, SF: surface, SW: satellite winds, UA: radiosondes.

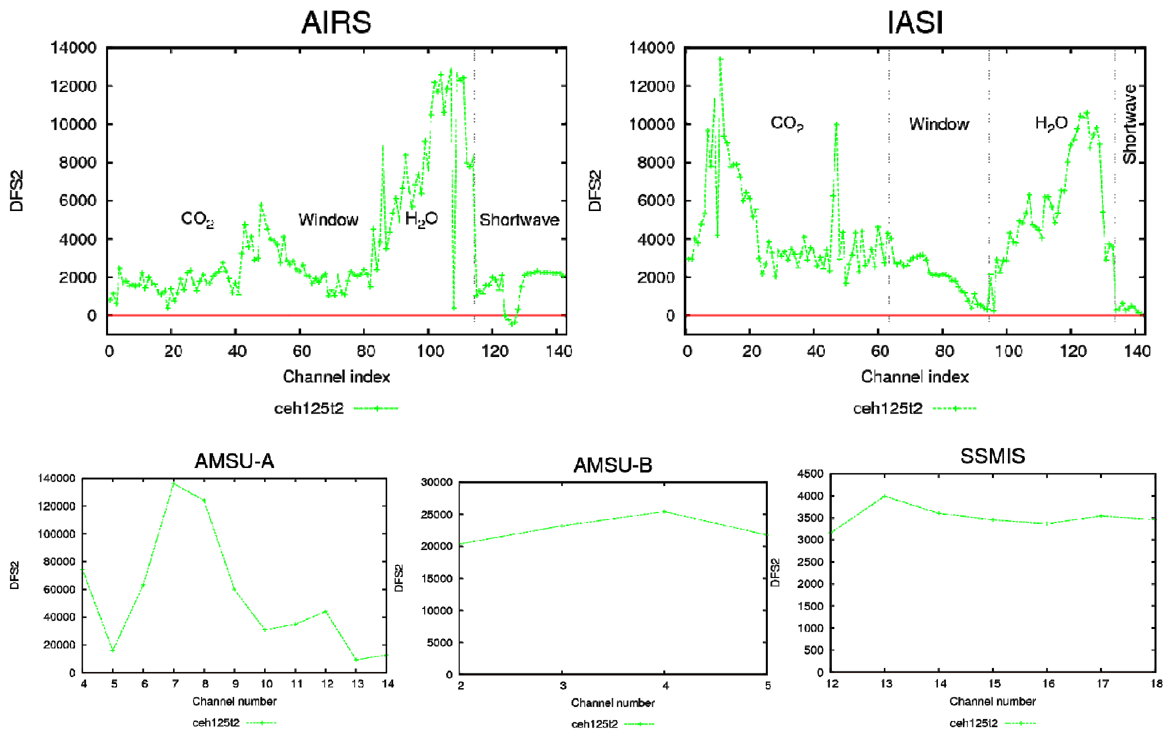

Fig. 6 : DFS per channel for AIRS (top left) and IASI (top right). See Table 1 for frequencies corresponding to channel index. DFS shown for AMSU-A, AMSU-B+MHS, and SSMIS, respectively, on lower panels.

DEGREES OF FREEDOM FOR SIGNAL

We used the approach of Lupu et al., 2011 to estimate the impact of observations based on Degrees of Freedom for Signal (DFS) from a cycle (CEH125T2) including the new channels and revised observation errors. DFS is defined by $E<(A-P)R^{-1}(O-A)>$ where R is the assigned observation error covariance matrix. Since DFS is based on analysis, observations and background quantities, the impact can be interpreted as the relative weight of each data type in the analysis and short term forecasts. Fig. 5 shows the number of observations per family over a period of 23 days and the corresponding DFS (DFS_2 represents DFS without division by the total number of observations N, including all data types). Fig. 6 shows DFS_2 pertaining to AIRS and IASI channels. It is seen that largest DFS pertain to aircrafts and radiosonde data, in good part due to their low observation errors and high vertical resolution. AMSU-A has the largest DFS for radiances, followed closely by IASI and AIRS. That result seems correlated with their respective number of observations. Fig. 6 shows that AIRS and IASI have similar DFS for water vapor channels. IASI is superior in the CO_2 band (low channel index). These results are expected from the corresponding differences seen in Fig. 3 for std(O-P). AMSU-A DFS confirm the higher impact from mid-tropospheric channels 6-9 in comparison to lowest and highest peaking channels. There are no significant DFS differences among various AMSU-B or SSMI/S channels.

CONCLUSION

Environment Canada is planning to move from 4DVar to EnVar in 2014. This provided an opportunity to review key aspects of radiance assimilation: channel selection, bias correction, and observation error. Although not explicitly shown here, the impact of radiance assimilation is as strong in EnVar as in 4DVar. Based on data denial experiments, the impact of infrared radiances appears relatively modest, but it is very large in the absence of microwave data. Similarly, the impact of microwave data is perceived as much larger in the absence of infrared data, evidencing the strong synergy between the two data types. Doubling the number of AIRS and IASI channels resulted in a clear positive impact in the Southern Hemisphere. It is planned to proceed with a similar approach and channel selection for the assimilation of Cris radiances from Suomi and IASI radiances from Metop-B, and to consider explicitly the interchannel error correlation. EnVar opens interesting avenues for the assimilation of surface sensitive channels over land because the background error correlation between surface temperature and atmospheric variables is locally available. This is the subject of an ongoing investigation.

REFERENCES

Buehner, M., J. Morneau, and C. Charette, 2013. Four-dimensional ensemble-variational data assimilation for global deterministic prediction. *Nonlin. Processes. Geophys*., **20**, 669-682.

Daescu, D. N., and R. H. Langland, 2013. Error covariance sensitivity and impact evaluation with adjoint 4D-Var: theoretical aspects and first applications to NAVDAS-AR. *Quart. J. Roy. Meteor. Soc*., **139**, 226-241.

Desroziers, G., L. Berre, B, Chapnik, and P. Poli, 2005. Diagnosis of observation, background, and analysis error statistics in observation space. *Quart. J. Roy. Meteor. Soc*., **131**, 3385-3396.

Garand, L., S. Heilliette, and M. Buehner, 2007. Interchannel error correlation associated with AIRS radiance observations: inference and impact in data assimilation. J*. Appl. Meteor. Climatol*., **46**, 714-725.

Gauthier, P., M. Tanguay, S. Laroche, S. Pellerin, and J. Morneau, 2007 : Extension of 3DVAR to 4DVAR: Implementation of 4DVAR at the Meteorological Service of Canada. *Mon. Wea. Rev.,* **135**, 2339-2354.

Houtekamer, P. L., X. Deng, H. L. Mitchell, S-J. Baek, and N. Gagnon, 2013. Higher resolution in an operational Ensemble Kalman Filter. *Mon. Wea. Rev*., **141**, in press.

Lupu, C., P. Gauthier, and S. Laroche, 2011. Evaluation of the impact of observations on analyses in 3D- and 4D-Var based on information content.